Global Image Registration by Fast Random Projection

Hayato Itoh[1], Shuang Lu[1], Tomoya Sakai[2], and Atsushi Imiya[3]

[1] School of Advanced Integration Science, Chiba University
Yayoicho 1-33, Inage-ku, Chiba, 263-8522, Japan
[2] Department of Computer and Information Sciences, Nagasaki University
Bunkyo-cho, Nagasaki, Japan
[3] Institute of Media and Information Technology, Chiba University
Yayoicho 1-33, Inage-ku, Chiba, 263-8522, Japan

Abstract. In this paper, we develop a fast global registration method using random projection to reduce the dimensionality of images. By generating many transformed images from the reference, the nearest neighbour based image registration detects the transformation which establishes the best matching from generated transformations. To reduce computational cost of the nearest nighbour search without significant loss of accuracy, we first use random projection. To reduce computational complexity of random projection, we second use spectrum-spreading technique and circular convolution.

1 Introduction

In this paper, we develop a fast global-image-registration algorithm using fast random projection [1,2,3].

Image registration overlays two or more template images, which are same sense observed at different times, from different viewpoints, and/or by different sensors, on a reference image. In general, there are parallel, rotation, scaling, and shearing spatial relationships between the reference image and template images. Therefore, image registration is a process to estimate these geometric transformations that transform all points or most points of the template images to points of the reference image. To estimate these spatial transformations, various methods are developed [4,5]. Image registration method generally classified into local image registration and global image registration.

For global alignment images, linear transformation

$$\boldsymbol{x}' = \boldsymbol{A}\boldsymbol{x} + \boldsymbol{b}. \tag{1}$$

which minimises the criterion

$$D(f, g) = \int_{\mathbb{R}^2} |f(\boldsymbol{x}) - g(\boldsymbol{x}')| d\boldsymbol{x}, \tag{2}$$

for a reference image $f(\boldsymbol{x})$ and the template image $g(\boldsymbol{x})$, is used to relate two images.

G. Bebis et al. (Eds.): ISVC 2011, Part I, LNCS 6938, pp. 23–32, 2011.

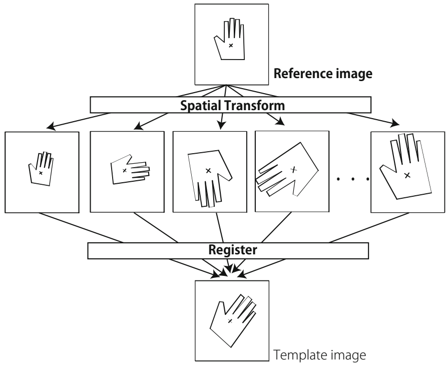

Fig. 1. Affine Transformation and Flow of Global Registration

For sampled affine transforms $\{\boldsymbol{A}_i\}_{i=1}^{m}$ and translation vectors $\{\boldsymbol{b}_j\}_{j=1}^{m}$, We generate transformed reference images such that

$$g^{ij} = g(\boldsymbol{A}_i\boldsymbol{x} + \boldsymbol{b}_j), i, j = 1, 2, \cdots, m. \tag{3}$$

Then, minimisation of R in eq. (2) is achieved by computing the criterion $\tilde{R}$

$$R = \min_{ij} \sum_{p,q=1}^{N} |f_{pq} - g_{pg}^{ij}| \tag{4}$$

where f_{pq} and g_{pq}^{ij} are discrete version of f and g^{ij}. We can use the nearest neighbour search (NNS) to find minimiser

$$g_*^{ij} = arg\left\{\min_{ij} \sum_{p,q=1}^{N} |f_{pq} - g_{pg}^{ij}|\right\}. \tag{5}$$

Figure 1 shows the procedure of global registration

The simplest solution to the NNS problem is to compute the distance from the query point to every other point in the database, preserving track of the "best so far." This algorithm, sometimes referred to as the naive approach, has a computational cost $\mathcal{O}(Nd)$ where N and d are the cardinality of a set of points in a metric space and the dimensionality of the metric space, respectively. In this paper, using the efficient random projection, We introduce a method to reduce the computational cost of this primitive of the NNS-based image registration.

2 Random Projection

Setting $E_D(A)$ to be the expectation of the event A on the domain D, for $k \ll n$ from $\boldsymbol{u} \in \mathbb{R}^n$, we compute the vector $\boldsymbol{v} \in \mathbb{R}^k$ such that

$$\boldsymbol{v} = \sqrt{\frac{n}{k}}\boldsymbol{R}^T\boldsymbol{u}, \quad E_{\mathbb{R}^k}(|\boldsymbol{v}|^2) = E_{\mathbb{R}^n}(|\boldsymbol{u}|^2), \tag{6}$$

where $\boldsymbol{R}$ is a uniform random orthonormal matrix and the scale $\sqrt{\frac{n}{k}}$ ensures the expected squared length of $\boldsymbol{v}$ equal to the squared length of $\boldsymbol{u}$. The transform of eq. (6) is called the random projection [6]. The random projection approximately preserves pairwise distances with high probability. The Johnson-Lindenstrauss lemma describes this geometric property.

Lemma 1. *(**Johnson − Lindenstrauss**) [7] For any $\frac{1}{2} > \epsilon > 0$, and any set of points X in $\mathbb{R}^n$, setting $k \geq \frac{4}{\epsilon^2/2-\epsilon^3/3}\log n$, every pair $\boldsymbol{u}$ and $\boldsymbol{v}$ satisfies the relation*

$$(1-\epsilon)|\boldsymbol{u}-\boldsymbol{v}|^2 \leq |f(\boldsymbol{u}) - f(\boldsymbol{v})|^2 \leq (1+\epsilon)|\boldsymbol{u}-\boldsymbol{v}||^2 \tag{7}$$

with probability at least $\frac{1}{2}$, where $f(\boldsymbol{u})$ and $f(\boldsymbol{v})$ are the projections of $\boldsymbol{u}$ and $\boldsymbol{v}$, respectively.

If the projection matrix $\boldsymbol{R}$ is a random orthonormal matrix, that is, each entry of the random matrix is selected independently from the standard normal distribution $N(0,1)$ with mean 0 and variance 1, we have the next lemma [8].

Lemma 2. *Let each entry of an $n \times k$ matrix $\boldsymbol{R}$ be chosen independently from N(0,1). Let $\boldsymbol{v} = \frac{1}{\sqrt{k}}\boldsymbol{R}^T\boldsymbol{u}$ for $\boldsymbol{u} \in \mathbb{R}^n$. For any $\epsilon > 0$,*
(1)$\boldsymbol{E}(|\boldsymbol{v}|^2) = |\boldsymbol{u}|^2$.
(2)$\boldsymbol{P}(|\boldsymbol{v}|^2 - |\boldsymbol{u}|^2| \leq \epsilon||u||^2) < 2e^{-(\epsilon^2-\epsilon^3)\frac{1}{4}}$.

Figure 2 shows the distance preserving property of the random projection from $\mathbb{R}^3$ to $\mathbb{R}^2$. Two points P_1' and P_2' in 3-dimensional space correspond to points P_1 and P_2, respectively in 2-dimensional space after random projection.

Using these lemmas, we can compress images using the Random projection. By expressing an $(n \times n)$-pixel image as an $(n \times n)$ matrix $\boldsymbol{A} = (\boldsymbol{a}_1, \boldsymbol{a}_1, \ldots, \boldsymbol{a}_n)$ where $\boldsymbol{a}_i \in \mathbf{R}^n$, we first transform $\boldsymbol{A}$ to $\boldsymbol{U}$,

$$\boldsymbol{u} = (\boldsymbol{a}_1^\top, \boldsymbol{a}_1^\top, \cdots, \boldsymbol{a}_n^\top)^\top \in \mathbf{R}^{n^2}, \tag{8}$$

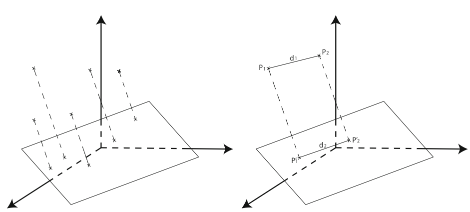

Fig. 2. Geometry of random projection. (a) Random Projection from 3D-space to 2D-space. (b) 2 points P_1' and P_2' in 3-dimensional space correspond to points P_1 and P_2, respectively in 2-dimensional space after random projection.

Using a random projection matrix $\boldsymbol{R} \in \mathbf{R}^{k^2 \times n^2}$ which satisfies the relation $N(0,1)$, we compute

$$\sqrt{\frac{1}{k}}\boldsymbol{R}^\top \boldsymbol{u} = \boldsymbol{v} = \left(\boldsymbol{v}_1^\top, \boldsymbol{v}_2^\top, \cdots, \boldsymbol{v}_k^\top\right)^\top \tag{9}$$

and transform $\boldsymbol{v}$ to

$$\boldsymbol{B} = \begin{pmatrix} v_1 & v_{k+1} & v_{2k+1} & \cdots & v_{k(k-1)} \\ \vdots & \vdots & \vdots & \ddots & \vdots \\ v_k & v_{2k} & v_{3k} & \cdots & v_{kk} \end{pmatrix} \in \boldsymbol{R}^{k \times k}, \tag{10}$$

Then, we obtain compressed image $\boldsymbol{B}$ from image $\boldsymbol{A}$.

Setting $\overline{f}$ and $\overline{g^{ij}}$ to be the random projection of the reference and template images, respectively, and

$$\overline{g}_*^{ij} = arg\left\{\min_{ij} \sum_{p,q=1}^{N} |\overline{f_{pq}} - \overline{g_{pg}^{ij}}|\right\}, \tag{11}$$

these lemmas imply the relations

$$P(|\overline{g_*^{ij}} - g_*^{ij}| \leq \varepsilon) > 1 - \delta, \tag{12}$$

for small positive numbers ε and δ, where $P(A)$ is the probability of the event A. Using this property, first we reduce the computational cost of the NNS search for the global registration of image.

3 Efficient Random Projection

Setting $\boldsymbol{w} = (w_1, \ldots, w_k)^\top$ to be an independent stochastic vector such that $E_{\mathbb{R}^k}[\boldsymbol{w}] = 0$, we have the relation $E_{\mathbb{R}^{k\times k}}[\boldsymbol{w}\boldsymbol{w}^\top] = \gamma^2 \boldsymbol{I}$. Furthermore, setting the $(i-1)$-time shifting of $\boldsymbol{w}$ to be

$$\boldsymbol{c_i} = (w_i, \ldots, w_k, w_1, \ldots, w_{i-1})^\top, \tag{13}$$

we define the matrix

$$\boldsymbol{C} = \begin{bmatrix} \boldsymbol{c}_1^\top \\ \vdots \\ \boldsymbol{c}_k^\top \end{bmatrix} = \begin{bmatrix} w_1 & w_2 & \cdots & w_{k-1} & w_k \\ w_2 & w_3 & \cdots & w_k & w_1 \\ \vdots & \vdots & \ddots & \vdots & \vdots \\ w_k & w_1 & \cdots & w_{k-2} & w_{k-1} \end{bmatrix}. \tag{14}$$

Since

$$E_{\mathbb{R}}(\boldsymbol{c_i}^\top \boldsymbol{c_j}) = \{ \begin{matrix} \gamma^2 d & (i = j) \\ 0 & (i \neq j) \end{matrix} \tag{15}$$

we have the relation

$$E_{\mathbb{R}}[|\boldsymbol{y}|_2^2] = E_{\mathbb{R}}[\sum_{i=1}^{k}(\boldsymbol{c}_{\boldsymbol{i}}^\top \boldsymbol{x})^2] = \sum_{i=1}^{k} \boldsymbol{x}^\top E_{\mathbb{R}^{k\times k}}[\boldsymbol{c}_{\boldsymbol{i}}\boldsymbol{c}_{\boldsymbol{i}}^\top]\boldsymbol{x} = \sum_{i=1}^{k} \boldsymbol{x}^\top \gamma^2 \boldsymbol{I}\boldsymbol{x} = k\gamma^2|\boldsymbol{x}|^2. \tag{16}$$

We set $\gamma = 1/\sqrt{k}$.

Setting $\boldsymbol{s} = (s_1, \ldots, s_k)^\top$ to be be an independent stochastic vector such that $E_{\mathbb{R}}[\boldsymbol{s}] = 0$ and $E_{\mathbb{R}^{k\times k}}[\boldsymbol{s}\boldsymbol{s}^\top] = \sigma^2\boldsymbol{I}$, a dense vector $\boldsymbol{\zeta}$ is computed as

$$\boldsymbol{\zeta} = \boldsymbol{s} \odot \boldsymbol{x} = [\boldsymbol{S}]\boldsymbol{x}, \tag{17}$$

from a sparse vector $\boldsymbol{x}$ where $[\boldsymbol{S}]$ is the diagonal matrix whose diagonals are $\{s_i\}_{i=1}^k$ fro $d \le n$. Then, we compute

$$\boldsymbol{y} = \boldsymbol{C}[\boldsymbol{S}]\boldsymbol{x} \tag{18}$$

from a sparse vector $\boldsymbol{x}$, where $[\boldsymbol{S}]$ is the diagonal matrix whose diagonals are $\{s_i\}_{i=1}^k$ for $k \le n$. The expectation of the norm is

$$E_{\mathbb{R}^k}[|\boldsymbol{y}|_2^2] = k\gamma^2\sigma^2|x|_2^2. \tag{19}$$

To preserve $E[|\boldsymbol{y}|_2^2] = |\boldsymbol{x}|_2^2$, we set $\gamma = 1/\sqrt{k}$ and $\sigma = 1$. Since $\boldsymbol{C\eta}$ is achieved by the cyclic convolution between $\boldsymbol{c}_i$ and $\boldsymbol{\eta}$, we can compute $\boldsymbol{C}[\boldsymbol{S}]\boldsymbol{x}$ using the Fast Fourier Transform. These algebraic property derive the next theorem.

Theorem 1. *The vector $\boldsymbol{x}$ is projected to the vector $\boldsymbol{y}$ using $O(d)$ memory area and $O(nd\log d)$ calculation time.*

4 Numerical Examples

Using the effective random projection proposed in the previous section [3], we propose a fast algorithm for global image registration. The flow charts are shown in Fig. 3. We evaluated performance of our method using data set of [9].

We first numerical accuracy of the algorithm assuming that the transforms are rotations around the centroid of images. In this case we can set $\boldsymbol{b}_j = 0$. Using a reference image A0 in Fig. 4 and seven images for three template images A, B, C, and D in Figs. 4 and 5. We have evaluated the rotation angle and the overlapping ratio $r = \min \tilde{R}/M$, where $M = \sum_{p,q=1}^{n} |f_{pq}|$, for each result. Table 1 shows the results. The results show that the method detects rotation angles with sufficient overlapping ratio.

Next, we show the computational cost the method according to the dimension of the original images. Figures 6(a) and 6 (b) show the relation between accuracy of the estimated parameters against the dimensions of the projected images and computation times of the NNS after the efficient random projection. These graphs show that in an appropriate dimension, the algorithm preserves speed of computation and accuracy of the results.

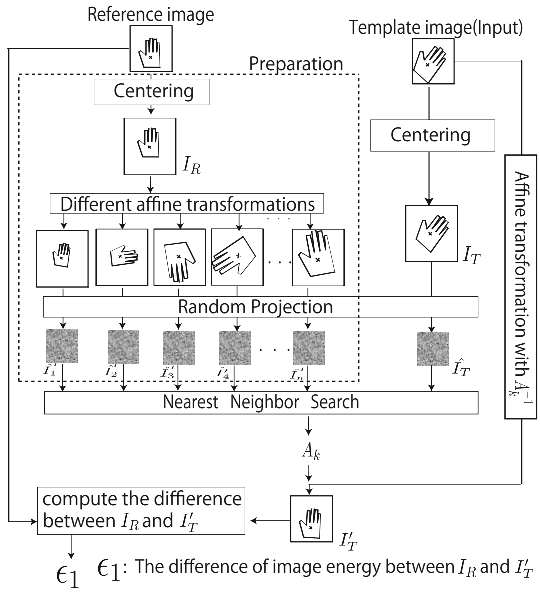

Fig. 3. Algorithm Flow

Table 1. Numerical Result for Rotation Images. $R = \min_{ij} \sum_{p,q=1}^{N} |f_{pq} - g_{pg}^{ij}$— and $M = \sum_{p,q=1}^{N} |f_{pq}|$.

Ground Truth	0	5	10	15	30	60	180
Reference	A0	A0	A0	A0	A0	A0	A0
Template	A0	A5	A10	A15	A30	A60	A180
estimation	0	5	10	15	30	60	180
min R/M	0.0007688	0.0130	0.0128	0.0129	0.0125	0.0125	0.0007688
Reference	A0	A0	A0	A0	A0	A0	A0
is Template	B0	B5	B10	B15	B30	B60	B180
estimation	0	5	10	15	30	60	180
min R/M	0.2008	0.1973	0.1971	0.1972	0.1973	0.1972	0.2008
Reference	A0	A0	A0	A0	A0	A0	A0
Template	C0	C5	C10	C15	C30	C60	C180
estimation	359	4	10	15	30	60	180
min R/M	0.2694	0.2669	0.2682	0.2682	0.2682	0.2682	0.2694
Reference	A0	A0	A0	A0	A0	A0	A0
Template	D0	D5	D10	DS15	D30	D60	D180
estimation	2	7	9	14	29	59	183
min R/M	0.4794	0.4760	0.4800	0.4798	0.4800	0.4796	0.4825

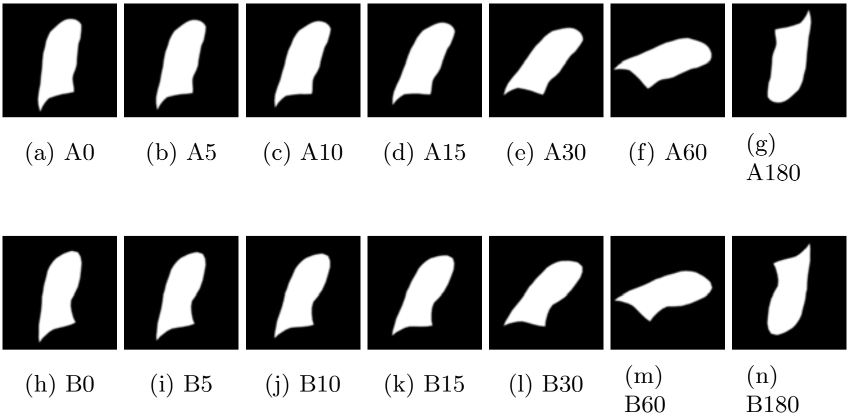

Fig. 4. Test Images 1

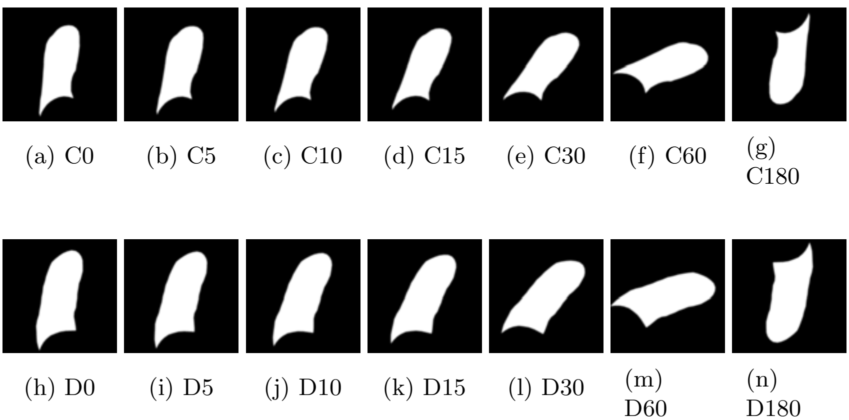

Fig. 5. Test Images 2

Finally, we show the registration results under various dimensionality reduction. Figure 7 shows results of registration under various dimensionality reduction in random projection. Equation (20) shows the estimated affine transformations under various dimensionality reduction in random projection. The estimated parameters in matrix forms are

$$\boldsymbol{A}_{16384} = \begin{pmatrix} 0.8572 & -0.5150 & 0 \\ 0.5150 & 0.8572 & 0 \\ 0 & 0 & 1 \end{pmatrix}, \ \boldsymbol{A}_{8192} = \begin{pmatrix} 0.8660 & -0.5000 & 0 \\ 0.5000 & 0.8660 & 0 \\ 0 & 0 & 1 \end{pmatrix},$$

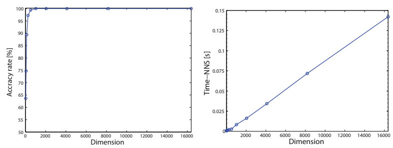

(a) Relationship between dimension and accuracy

(b) Relationship between dimension and the NNS

Fig. 6. Computational Costs and Accuracy of the Method

$$\boldsymbol{A}_{4096} = \begin{pmatrix} 0.8746 & -0.4848 & 0 \\ 0.4848 & 0.8746 & 0 \\ 0 & 0 & 1 \end{pmatrix}, \ \boldsymbol{A}_{2048} = \begin{pmatrix} 0.8572 & -0.5150 & 0 \\ 0,5150 & 0.8572 & 0 \\ 0 & 0 & 1 \end{pmatrix},$$
$$\boldsymbol{A}_{1024} = \begin{pmatrix} 0.8829 & -0.4695 & 0 \\ 0.4695 & 0.8829 & 0 \\ 0 & 0 & 1 \end{pmatrix}, \ \boldsymbol{A}_{512} = \begin{pmatrix} 0.8746 & -0.4848 & 0 \\ 0.4848 & 0.8746 & 0 \\ 0 & 0 & 1 \end{pmatrix},$$
$$\boldsymbol{A}_{32} = \begin{pmatrix} 0.9063 & -0.4226 & 0 \\ 0.4226 & 0.9063 & 0 \\ 0 & 0 & 1 \end{pmatrix}, \ \boldsymbol{A}_{16} = \begin{pmatrix} -0.9063 & 0.3432 & 0 \\ -0.3432 & -0.9063 & 0 \\ 0 & 0 & 1 \end{pmatrix}, \tag{20}$$

where

$$\boldsymbol{A}_k = \begin{pmatrix} \boldsymbol{A}_i & \boldsymbol{b}_j \\ \boldsymbol{o}^\top & 0 \end{pmatrix}. \tag{21}$$

Therefore, in these experiments $\boldsymbol{b}_j = \mathbf{0}$ and $P(|\boldsymbol{A}_i^\top \boldsymbol{A} - \boldsymbol{I}|_2 < \varepsilon) = 1 - \delta$ for the Frobenius norm $|\boldsymbol{A}|_2$ of the matrix $\boldsymbol{A}$. Table 2 lists the estimated angles for various dimensional random-projected images.

Table 2. Estimeted Angles for Various Dimensional Images

Grount Truth	30	30	30	30	30	30	30	30
Estimated Angle	31	30	29	31	28	29	25	200
Dimension	16384	8192	4096	2048	1024	512	32	16

These results show that if the dimension of the projected subspace is too small, the registration will be failed and the estimated affine parameter maybe not accurate. Furthermore, if the projected the dimension of subspace is not too small, the computational cost of global registration can be reduced by the efficient random projection without significant loss of accuracy.

The complexities of the naive and fast random projection methods are shown in table 3 These relations show that in total the method reduces the computational time of fot global registration with random projection.

(a) Reference D0 (b) Template D30

(c) Result: to 16384 dimension (d) Result: to 8192 dimension (e) Result: to 4096 dimension (f) Result: to 1024 dimension (g) Result: to 512 dimension (h) Result: to 32 dimension (i) Result: to 16 dimension

Fig. 7. Result Images for Various Dimensionality Reduction. Image A and $D30$ are used.

Table 3. Theoretical Comparison Computational Complexities. (a) memeory area for the random matrix. (b) memeory area for the random vectors.

	Computation Time of Projection	Memory of Operation	Memory of Projected Data	Pre-Process of NNS	NNS
naive	$O(nd \log n)$	$O(d \log n)$ (a)	kn		n
fast	$O(nd \log d)$	$O(d)$ (b)	kn	$O(n \log n)$	$O(\log n)$
ratio(n:f)	$\log n : \log d$	$d \log n : d$	$1 : 1$	$0 : n \log n$	$n : \log n$

5 Conclusions

In this paper, using a fast random projection, we developed an efficient algorithm that establishes global image registration. We introduced to use spectrum spreading and circular convolution to reduce computational cost of random projection.

After establishing global registration, we apply elastic registration by solving the minimisation problem[1]

[1] This is a discrete expression of variational image registration which is achieved by minimising the criterion

$$J(\boldsymbol{u}) = \int_{\mathbb{R}^2} \{(f(\boldsymbol{x} - g(\boldsymbol{x} + \boldsymbol{u}))^2 + \lambda Q(\boldsymbol{u})\} d\boldsymbol{x}.$$

$$J(u,v) = \sum_{p,q=1}^{N} \left\{ |f_{pq} - [g^{ij}_{*(p+u,q+v)})]_{pq}|^2 + \lambda[Q(u,v)]_{pq} \right\} \tag{22}$$

for an appropriate prior Q, where $[Tf_{mn}]_{pq}$ expresses resampling of f_{mn} after applying the transformation T to f_{pq}.

Extensions of the method to range images and 3D volumetric images are straight forward.

Acknowledgement. This research was supported by "Computational anatomy for computer-aided diagnosis and therapy: Frontiers of medical image sciences" funded by Grant-in-Aid for Scientific Research on Innovative Areas, MEXT, Japan, Grants-in-Aid for Scientific Research founded by Japan Society of the Promotion of Sciences and Grant-in-Aid for Young Scientists (A), NEXT, Japan.

References

1. Healy, D.M., Rohde, G.K.: Fast global image registration using random projection. In: Proc. Biomedical Imaging: From Nano to Macro, pp. 476–479 (2007)
2. Sakai, T.: An efficient algorithm of random projection by spectrum spreading and circular convolution, Inner Report IMIT Chiba University (2009)
3. Sakai, T., Imiya, A.: Practical algorithms of spectral clustering: Toward large-scale vision-based motion analysis. In: Wang, L., Zhao, G., Cheng, L., Pietikäinen, M. (eds.) Machine Learning for Vision-Based Motion Analysis Theory and Techniques. Advances in Pattern Recognition. Springer, Heidelberg (2011)
4. Zitová, B., Flusser, J.: Image registration methods: A Survey. Image Vision and Computing 21, 977–1000 (2003)
5. Modersitzki, J.: Numerical Methods for Image Registration. In: CUP (2004)
6. Vempala, S.S.: The Random Projection Method. DIMACS, vol. 65 (2004)
7. Johnson, W., Lindenstrauss, J.: Extensions of Lipschitz maps into a Hilbert space. Contemporary Mathematics 26, 189–206 (1984)
8. Frankl, P., Maehara, H.: The Johnson-Lindenstrauss lemma and the sphericity of some graphs. Journal of Combinatorial Theory Series A 44, 355–362 (1987)
9. van Ginneken, B., Stegmann, M.B., Loog, M.: Segmentation of anatomical structures in chest radiographs using supervised methods: a comparative study on a public database. Medical Image Analysis 10, 19–40 (2006)